

High precision oxygen three-isotope analyses of anhydrous chondritic interplanetary dust particles

Daisuke NAKASHIMA^{1*}, Takayuki USHIKUBO¹, Michael E. ZOLENSKY², and Noriko T. KITA¹

¹WiscSIMS, Department of Geoscience, University of Wisconsin–Madison, Madison, Wisconsin 53706, USA

²Astromaterials Research and Exploration Science, NASA Johnson Space Center, Houston, Texas 77058, USA

*Corresponding author. E-mail: naka@geology.wisc.edu

(Received 08 June 2011; revision accepted 21 November 2011)

Abstract—Oxygen three-isotope ratios of three anhydrous chondritic interplanetary dust particles (IDPs) were analyzed using an ion microprobe with a 2 μm small beam. The three anhydrous IDPs show $\Delta^{17}\text{O}$ values ranging from -5‰ to $+1\text{‰}$, which overlap with those of ferromagnesian silicate particles from comet Wild 2 and anhydrous porous IDPs. For the first time, internal oxygen isotope heterogeneity was resolved in two IDPs at the level of a few per mil in $\Delta^{17}\text{O}$ values. Anhydrous IDPs are loose aggregates of fine-grained silicates (≤ 3 μm in this study), with only a few coarse-grained silicates (2–20 μm in this study). On the other hand, Wild 2 particles analyzed so far show relatively coarse-grained (\geq few μm) igneous textures. If anhydrous IDPs represent fine-grained particles from comets, the similar $\Delta^{17}\text{O}$ values between anhydrous IDPs and Wild 2 particles may imply that oxygen isotope ratios in cometary crystalline silicates are similar, independent of crystal sizes and their textures. The range of $\Delta^{17}\text{O}$ values of the three anhydrous IDPs overlaps also with that of chondrules in carbonaceous chondrites, suggesting a genetic link between cometary dust particles (Wild 2 particles and most anhydrous IDPs) and carbonaceous chondrite chondrules.

INTRODUCTION

Oxygen isotope ratios ($^{18}\text{O}/^{16}\text{O}$ and $^{17}\text{O}/^{16}\text{O}$) of extraterrestrial materials are known to show a wide variation, and many of them plot generally along a slope approximately one line in the oxygen three-isotope diagram, in which $^{18}\text{O}/^{16}\text{O}$ and $^{17}\text{O}/^{16}\text{O}$ ratios are converted to $\delta^{18}\text{O}$ and $\delta^{17}\text{O}$ (per mil deviations from Vienna Standard Mean Ocean Water). A significant amount of data has been published that range from -80‰ to $+200\text{‰}$ in $\delta^{18}\text{O}$ and $\delta^{17}\text{O}$ values, from bulk meteorites, Ca-Al-rich inclusions (CAIs), chondrules, meteorite matrix (e.g., Clayton et al. 1977; Clayton 1993; Kobayashi et al. 2003), cosmic-symplectite (COS) (Sakamoto et al. 2007), and solar wind collected by the Genesis Spacecraft (McKeegan et al. 2011). It has been suggested that the mass-independent isotope variation of oxygen among extraterrestrial materials originated from isotope selective photodissociation of CO induced by UV irradiation in the molecular cloud (Yurimoto and Kuramoto 2004) or in the protoplanetary disk (Lyons and Young 2005).

While these significant isotope anomalies have been obtained from the inner solar system materials, oxygen isotope ratios of outer solar system objects (beyond the asteroid belt) are still largely unknown. A missing piece of information on the oxygen isotope signature of the outer solar system was provided by particles collected from comet 81P/Wild 2 (The Stardust mission; Brownlee et al. 2006). A particle reported from comet 81P/Wild 2 consisted of refractory minerals and was similar to CAIs, especially those in some carbonaceous chondrites (Zolensky et al. 2006). The CAI-like Wild 2 particle (particle from track 25, Inti) showed oxygen isotope ratios similar to those of CAIs in chondrites (McKeegan et al. 2006). Nakamura et al. (2008, 2009) found ferromagnesian Wild 2 particles that are petrologically and chemically identical to chondrules in chondrites, and whose oxygen isotope ratios were similar to those of chondrules in carbonaceous chondrites. Ciesla (2007), among others, suggested a radial transport mechanism of the high temperature solids from the inner solar nebula to the outer solar nebula regions which could account for inner solar

system solids being captured by accreting cometary objects.

In addition to particles from Wild 2, which sampled a single comet, many of the interplanetary dust particles (IDPs) collected in Earth's stratosphere may have originated from short period comets (cf. Bradley 2003). These should have had atmospheric entry velocities of $>14 \text{ km s}^{-1}$, generally (but not universally) faster than those of asteroidal origin ($\sim 12 \text{ km s}^{-1}$; Jackson and Zook 1992). Brownlee et al. (1995) estimated atmospheric entry velocities of specific captured IDPs based on the degree of frictional heating deduced from solar-wind-implanted ^4He release patterns, and found that IDPs with atmospheric entry velocities of $>18 \text{ km s}^{-1}$ were dominated by anhydrous minerals (see also Joswiak et al. 2000), consistent with a primitive history. Most anhydrous chondritic porous IDPs (commonly referred as CP IDPs) show primitive characteristics, such as highly variable deuterium/hydrogen ratios that are thought to have cold molecular cloud origin (Messenger 2000) and high abundances of presolar silicate grains (e.g., Messenger et al. 2003). They often contain GEMS (glass with embedded metal and sulfide) grains that are a mineralogically disequilibrium assemblage of oxygen-rich, low-iron magnesium silicate glass embedded with nanometer-sized inclusions of FeNi metal and Fe-sulfides (Bradley 1994, 2003; Keller and Messenger 2011). These primitive characteristics and the loosely aggregated porous texture may be best explained if they originated from comets in which aqueous fluids were never generated (Bradley [2003] and references therein). As approximately 30,000–40,000 metric tons of dust particles, including anhydrous porous IDPs, are delivered to the Earth each year (Love and Brownlee 1993), the anhydrous porous IDPs are more accessible (and less altered by collection) than Wild 2 particles. Orbit computations have revealed the timing of dust delivery to the Earth from Earth-crossing comets, most recently from 26P/Grigg-Skjellerup and 73P/Schwassmann-Wachmann 3 (Messenger 2002, 2011). Thus, anhydrous porous IDPs are suitable samples to study outer solar system objects, and some of these may have known origins.

Oxygen in ferromagnesian crystalline silicates in anhydrous porous IDPs shows a narrow range of oxygen isotope ratios with $\Delta^{17}\text{O}$ ($=\delta^{17}\text{O} - 0.52 \times \delta^{18}\text{O}$) values $\sim -2\%$ (Aléon et al. 2009), which are similar to ferromagnesian crystalline silicate particles from comet Wild 2 (McKeegan et al. 2006; Nakamura et al. 2008; Nakashima et al. 2011a). Aléon et al. (2009) suggested a genetic relationship between the anhydrous porous IDPs and Wild 2 particles.

To further compare anhydrous IDPs to Wild 2 particles, we report oxygen isotope ratios of three

anhydrous IDPs (L2005 E36, L2005 F39, and L2005 Z17) that were previously studied for their mineralogy by Zolensky and Barrett (1994). Olivine in the three anhydrous IDPs shows a wide range of Fo# (Mg/[Mg + Fe] mole%; ~ 70 – 90 for E36, 60 – 100 for F39, and 50 – 90 for Z17; Zolensky and Barrett 1994). L2005 E36 and L2005 F39 are fragments of cluster IDPs L2005 #25 and L2005 #31 respectively; the latter IDP shows a large deuterium enrichment ($\delta D \sim +20,000\%$; Messenger 2000).

In the previous oxygen isotope studies of anhydrous porous IDPs, the samples were often pressed into gold foils (e.g., McKeegan 1987; Aléon et al. 2009). The disadvantage of this sample preparation technique is that the original petrologic texture is destroyed. Furthermore, the unpolished surface would produce a potential SIMS analytical bias due to surface topography (Kita et al. 2009). To avoid these problems, we remounted and polished the IDPs to obtain a flat sample surface, and followed the new analytical protocols developed for tiny particles using the multicollector ion microprobe at University of Wisconsin-Madison (Nakamura et al. 2008; Nakashima et al. 2011b).

ANALYTICAL PROCEDURES

Sample Preparation

The three anhydrous IDPs that we selected in this study were known to contain olivine and pyroxene crystals larger than 1 – $2 \mu\text{m}$ (Zolensky and Barrett 1994), which are large enough to be individually analyzed by SIMS. Before embedding in epoxy, the three IDPs were rinsed with freon and hexane to remove silicone oil, which is used for collecting IDPs in the stratosphere. Two IDPs (L2005 E36 and L2005 Z17; hereafter E36 and Z17) were embedded in small epoxy chips ($\sim 200 \mu\text{m} \times 100 \mu\text{m} \times$ few dozen micrometers) and another IDP (L2005 F39; hereafter F39) was mounted in a $200 \mu\text{m} \times 200 \mu\text{m}$ square top mesa of an epoxy potted butt with an 8 mm diameter. All these particles had a microtomed surface. Procedures for sample preparation are similar to those described in Nakashima et al. (2011b). Epoxy chips containing E36 and Z17 were individually placed on the center of epoxy disks (8 mm diameter and ~ 2 – 2.5 mm thickness) and fixed with a drop of epoxy resin (Fig. 1). Two San Carlos olivine standard grains (50 – $200 \mu\text{m}$ in longest diameter) were added to each disk, by leaning against the two side-walls of the epoxy chips (E36 and Z17) or $200 \mu\text{m}$ square epoxy mesa (F39) that contained the IDPs. Then, the surface of the epoxy disks (E36 and Z17) and epoxy rod (F39) were covered with new epoxy resin and cured. The covered surface was then ground and polished using

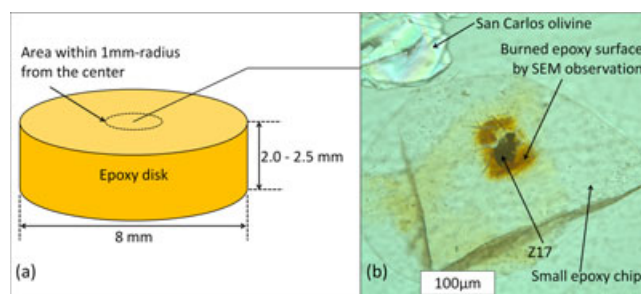


Fig. 1. Schematic drawing of an epoxy disk (a) and an optical microscope image (transmitted light) of IDP L2005 Z17 (b), which is located in an area within 1 mm radius from the center of the epoxy disk.

diamond lapping film and diamond suspension until both IDPs and standard grains were exposed on the flat surface. The epoxy rod was sliced to a thickness of approximately 2.5 mm from the final polished surface in order to fit in the special adaptor for the SIMS sample holder.

During the mounting of IDPs and San Carlos olivine standard grains in the epoxy disks, we carefully located them precisely within a 1 mm radius from the center of the epoxy disks (Fig. 1a). This is important for SIMS analysis, because instrumental mass fractionation occurs at the outside of the 1 mm radius from the center of the epoxy disks ($\geq \pm 0.5\%$ in $\delta^{18}\text{O}$; Nakashima et al. 2011b). We also carefully adjusted the height of San Carlos olivine standard grains to be above the original microtomed surface of the IDPs. In this way, the standard grains would be exposed to the surface of the final epoxy disk so that they could be analyzed repeatedly before and after the IDP analyses.

Electron Microscopy

The polished surface of the IDPs was observed using a scanning electron microscope (SEM; Hitachi S3400) with an energy-dispersive X-ray spectrometer (EDS) at University of Wisconsin-Madison, resulting in backscattered electron (BSE) and secondary electron (SE) imaging. Long periods of exposure of samples to the electron beam at high beam intensities would damage the epoxy resin surrounding IDPs, creating significant depressions or deformation. This topography or tilting of the sample surface could cause a significant instrumental mass fractionation in oxygen isotope ratios. Therefore, we tried to minimize the beam intensity and the total exposure time of SEM observation before the SIMS analysis. Detailed observation using SEM was done after ion microprobe analyses; at that time all SIMS pits were inspected. In addition to the Hitachi S3400 SEM, a Zeiss LEO1530 field emission (FE) SEM at Material Science

Center, University of Wisconsin-Madison was used to confirm the analyzed positions.

As mentioned earlier, IDP samples were cleaned with freon and hexane to remove silicone oil prior to sample mounting. Silicone oil mainly consists of Si, H, and O, so that a small amount of leftover oil could contaminate oxygen isotope analyses of the IDPs. We carefully examined fine-grained phases in the three IDPs using SEM-EDS so as to estimate the amount of phosphorous, which is used as an indicator of contamination of silicone oil in IDPs (Bradley et al. 2011). The EDS spectra of the fine-grained phases in the three IDPs did not show clear peaks of phosphorous, suggesting that contamination of silicone oil is not significant in the three IDPs.

Oxygen Isotope Analyses

The 8 mm epoxy disks that contain the IDPs were mounted in the sample holding disk (25 mm in diameter) with three holes (8mm in diameter), which was developed especially for high precision SIMS stable isotope analyses of cometary particles (Nakashima et al. 2011b). Oxygen isotope ratios of the three IDPs were analyzed with the CAMECA IMS-1280 ion microprobe at the WiscSIMS laboratory (Kita et al. 2009). The analytical conditions and measurement procedures were similar to those in Nakamura et al. (2008). A focused Cs^+ primary beam was set to approximately $1\ \mu\text{m} \times 2\ \mu\text{m}$ and intensity of approximately 3 pA. The $^{16}\text{O}^-$, $^{17}\text{O}^-$, and $^{18}\text{O}^-$ ions were detected simultaneously. Secondary ions of $^{16}\text{O}^-$ and $^{18}\text{O}^-$ were detected using Faraday cup (FC) and electron multiplier (EM) on the multiple collector trolleys, respectively, with mass resolving power (MRP) of 2200 (at 10% height). The EM at the ion optical axis and fixed position (mono collection detector) was used for detection of $^{17}\text{O}^-$ with MRP ~ 5000 (at 10% height). Intensities of $^{16}\text{O}^-$ were approximately 2×10^6 cps. The baselines of the multi-FC were measured during the presputtering (240 s) in respective analyses and used for data correction. The contribution of the tail of $^{16}\text{O}^1\text{H}^-$ to the $^{17}\text{O}^-$ signal was corrected by the method described in Heck et al. (2010). The uncertainties of the corrections (14% of corrected amounts) were added to the final error assignments for $\delta^{17}\text{O}$ and $\Delta^{17}\text{O}$ (see Heck et al. 2010).

Three to seven analyses were performed in individual IDPs, bracketed by eight analyses on the San Carlos olivine grains mounted in the same epoxy disks. External reproducibility of the San Carlos olivine grains was 0.9–1.5‰ for $\delta^{18}\text{O}$, 1.2–1.8‰ for $\delta^{17}\text{O}$, and 1.0–2.0‰ for $\Delta^{17}\text{O}$ (2 SD; standard deviation), which are assigned as analytical uncertainties of unknown samples (see Kita et al. 2009, 2010 for detailed explanations). We analyzed two low-Ca pyroxene (En97 and En85) standards (Kita

et al. 2010) in the same session for correction of instrumental bias of low-Ca pyroxene. Individual data were carefully examined after the inspection of SIMS pits using the SEM.

To evaluate the effects of epoxy potentially being present in fine-grained phases of anhydrous porous IDPs (E36 and F39), we analyzed epoxy resin and olivine standards in one disk, although the test was made under oxygen two isotope ($^{18}\text{O}/^{16}\text{O}$) analyses using 10 μm spots (primary beam intensity of ~ 2 nA) and multiple FC detectors, similar to the condition described in Kita et al. (2009). Analyses were made with variable proportions of epoxy and olivine mixtures in the analysis spots; from 100% (clean epoxy) to 0% (olivine). Data are shown in the Supporting Information section. These measurements of epoxy resulted in low $\delta^{18}\text{O}$ values (as low as -35‰). The secondary $^{16}\text{O}^-$ count rates from epoxy were only 1.2×10^8 cps, which was approximately one-twentieth of those of San Carlos olivine (2.6×10^9 cps). In the case of approximately 3 pA primary beam that yields secondary $^{16}\text{O}^-$ of 2×10^6 cps for olivine standard, the secondary $^{16}\text{O}^-$ count rates from epoxy are expected to be 1×10^5 cps. Because of the relatively low secondary oxygen ion yield from epoxy resin, the effect of epoxy contamination on the measured oxygen isotope ratios are probably not a significant factor in the analyses of fine-grained phase in the IDPs.

RESULTS

Petrology of Anhydrous IDPs

Figure 2 shows BSE images of the three IDPs (see also Zolensky and Barrett 1994). E36 is porous and consists of submicrometer silicates (Fig. 2a; mainly low-Ca pyroxene and olivine; Zolensky and Barrett 1994). Formerly, this IDP contained a large enstatite crystal ($\sim 10 \mu\text{m} \times 15 \mu\text{m}$) with Fe-Mg zoning (Zolensky and Barrett 1994). However, it was lost before the current sample preparation. F39 is also porous and consists of olivine and pyroxene (mostly low-Ca pyroxene) smaller than $3 \mu\text{m}$ (Fig. 2b). The surface of this IDP is partially underneath epoxy. This is because the microtomed surface of the IDP was slightly tilted against the polished surface. The two IDPs (E36 and F39) are porous, and for this reason, epoxy permeated into intercrystalline voids (Figs. 2d and 2e). The third IDP Z17 consists of low-Ca pyroxene grains larger than $2 \mu\text{m}$ up to $20 \mu\text{m}$, submicrometer silicate, and FeNi metal grains (detected by SEM-EDS; Fig. 2c). There are two kinds of fine-grained domains in Z17: dense and porous. The dense domain consists of submicrometer silicates (olivine and low-Ca pyroxene) that are packed together and are almost free of epoxy (Fig. 2f). In the porous domain,

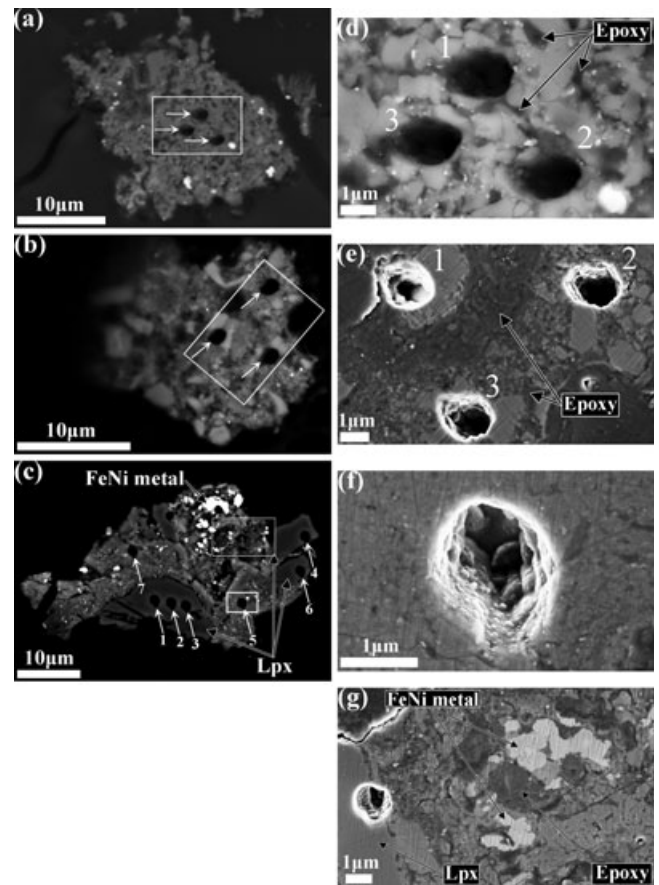


Fig. 2. BSE images of the surfaces of the three IDPs; (a) L2005 E36, (b) L2005 F39, and (c) L2005 Z17. Enlarged SE images show the SIMS pits in individual IDPs: (d) L2005 E36, (e) L2005 F39, and (f) L2005 Z17. Panel (g) shows the fine-grained porous domain in Z17. In panel (g), there is a hole at the edge of low-Ca pyroxene, which is a pit made by SIMS analysis that was aborted in the middle of measurement, because significant drift of isotope ratios occurred. White rectangles in the respective BSE images indicate the locations of panels (d), (e), (f), and (g). White arrows indicate SIMS pits in the IDPs. Numbers near the SIMS pits in panels (c), (d), and (e) correspond to SIMS analysis spot numbers in Table 1. Lpx = low-Ca pyroxene.

submicrometer silicates and FeNi metal loosely aggregate and the void spaces are filled with epoxy (Fig. 2g). The grain size of submicrometer silicate is estimated as approximately 100 nm to $1 \mu\text{m}$ from FE-SEM observation. SEM-EDS shows that the fine-grained dense domain around the SIMS pits (spots 5 and 7; Fig. 2c) is dominated by olivine rather than low-Ca pyroxene in various proportions (olivine makes up $> 90\%$ around spot 5 and $\sim 70\%$ around spot 7).

Previous TEM observations did not find GEMS grains in the three IDPs (Zolensky M. E. unpublished data). We also searched for GEMS grains in the three IDPs with FE-SEM using an example from Aléon et al.

Table 1. Oxygen isotope ratios and secondary ^{16}O count rates of three anhydrous IDPs, L2005 E36, F39, and Z17^{a,b,c}.

	Spot#	$\delta^{18}\text{O} \pm 2 \text{ SD} (\text{‰})$		$\delta^{17}\text{O} \pm 2\sigma (\text{‰})$		$\Delta^{17}\text{O} \pm 2\sigma (\text{‰})$	Target	^{16}O (10^6 cps)	OH correction (‰) ^d	
L2005	1					0.0	1.1	Fine-grained	2.06	0.4
E36	2					1.1	1.1	Fine-grained	2.20	0.4
	3					-2.8	1.1	Fine-grained	1.84	0.5
	Average					-0.6	0.8			
L2005	1					-2.1	1.1	Fine-grained	1.91	4.0
F39	2					-4.6	1.4	Fine-grained	2.07	7.2
	3					-2.5	1.0	Fine-grained	2.16	1.6
	Average					-3.0	0.6			
L2005	1	-1.9	1.5	-4.5	1.8	-3.5	2.0	Low-Ca px	1.73	0.1
Z17	2	-3.3	1.5	-6.0	1.8	-4.3	2.0	Low-Ca px	1.78	0.1
	3	-1.0	1.5	-5.3	1.8	-4.8	2.0	Low-Ca px	1.67	0.1
	4	-6.2	1.5	-7.1	1.8	-3.9	2.0	Low-Ca px	1.88	0.2
	5					-0.9	2.0	Fine-grained	2.12	0.8
	6	-2.0	1.5	-6.3	1.8	-5.2	2.0	Low-Ca px	1.72	0.1
	7					0.0	2.0	Fine-grained	2.70	0.6
	Average	-2.9	0.7	-5.8	0.8	-4.3	0.9	Low-Ca px		
	Average					-0.4	1.4	Fine-grained		

^aThe uncertainties associated with $\delta^{18}\text{O}$ are external reproducibility (2 SD) of eight sets of bracketing analyses of San Carlos olivine standard grains which are embedded with the IDPs in epoxy disks, while confidence errors (95%; 2σ) associated with $\delta^{17}\text{O}$ and $\Delta^{17}\text{O}$ include external reproducibility and uncertainty of hydride correction (Heck et al. 2010).

^bInstrumental bias correction was not applied for the fine-grained phases in E36, F39, and Z17 (see text).

^cBold-faced numbers are average values and twice the standard error of the mean (2 SE).

^dHydride correction (‰) = $^{16}\text{O}^1\text{H}^- \text{ intensity} / [^{17}\text{O}^- \text{ intensity} \times (^{17}\text{O}^- \text{ tail} / ^{17}\text{O}^- \text{ intensity})] \times 1000$; $^{17}\text{O}^- \text{ tail} / ^{17}\text{O}^- \text{ intensity} = 1.3 \times 10^{-5}$.

(2009), without success. Although the absence of GEMS might indicate that the fine-grained phases in these IDPs are equilibrated aggregates (Bradley 1995), Zolensky and Barrett (1994) reported a wide range of Fo# in olivine in the three IDPs (see the Introduction). This indicates that these three IDPs are truly unequilibrated. Therefore, it is likely that the three IDPs were originally depleted in GEMS grains compared to typical anhydrous porous IDPs, but we cannot completely rule out the presence of GEMS grains in the three IDPs.

Oxygen Isotope Ratios in IDPs

We obtained a total of 13 spot analyses from three IDPs. The full data table is shown in the Supporting Information section, and a summary of the analyses is shown in Table 1.

Coarse Low-Ca Pyroxene in Z17

In Z17, five analyses were made in low-Ca pyroxene grains that are as large as several micrometers to 20 μm . The inspection of SIMS pits using the SEM indicates that the individual spots are within low-Ca pyroxene grains and do not overlap with other domains. Secondary ion intensities were stable and as high as those of the San Carlos olivine standards. The interference correction from $^{16}\text{O}^1\text{H}^-$ was smaller than 0.2 ‰ (Table 1). These

data are reproducible within analytical uncertainties and plot between the carbonaceous chondrite anhydrous mineral (CCAM) and Young and Russell (Y&R) lines (Clayton et al. 1977; Young and Russell 1998). The average and 2 SE (standard error of the mean) of $\delta^{18}\text{O}$, $\delta^{17}\text{O}$, and $\Delta^{17}\text{O}$ values of five analyses are $-2.9 \pm 0.7\text{‰}$, $-5.8 \pm 0.8\text{‰}$, and $-4.3 \pm 0.9\text{‰}$, respectively. One data point (spot 4; Fig. 3; Table 1) slightly deviates toward low $\delta^{18}\text{O}$ compared to the other low-Ca pyroxene data. However, spot 4 appears to hit the edge of the low-Ca pyroxene grain, which may have induced slight mass-dependent instrumental fractionation (Kita et al. 2009).

Analysis of Fine-Grained Phases

Eight analyses were made in fine-grained phases in three IDPs. The inspection of SIMS pits using the SEM indicates that the individual spots were all mixtures of submicrometer olivine and pyroxene grains (plus epoxy in E36 and F39), as we did not find GEMS. We noticed that the secondary $^{16}\text{O}^-$ intensity during the analyses of fine-grained phases was 5–50% higher than those of the olivine standard. Secondary ion intensities fluctuated during individual analyses. Often, raw $\delta^{18}\text{O}$ values drifted more than 15 ‰ toward lower values during a single analysis, which was never observed during the analyses of standards and coarse low-Ca pyroxene grains

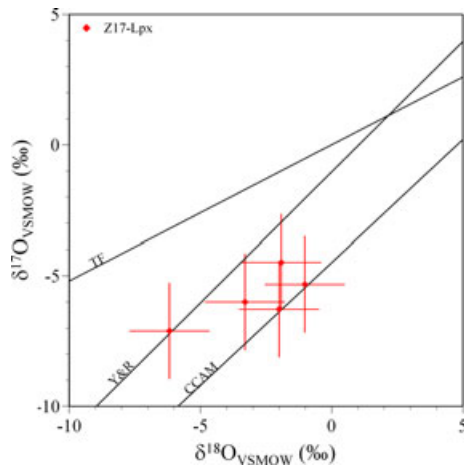


Fig. 3. Oxygen isotope ratios of coarse low-Ca pyroxene in IDP L2005 Z17. TF, Y&R, and CCAM represent the terrestrial fractionation line, the Young & Russell line, and the carbonaceous chondrite anhydrous mineral line.

in Z17. It is possible that the conditions of sputtering of the fine-grained phases were very different from that of single mineral analysis. It is possible that heterogeneous sputtering rates resulted from the mixture of multiple minerals. Instrumental mass fractionation during the analysis of fine-grained phases would be variable from spot to spot, and the matrix corrections using mineral standards might not be completely successful. However, this instrumental mass fractionation occurs in a mass-dependent manner, and therefore the $\Delta^{17}\text{O}$ values from these fine-grained phase analyses would not be affected. Indeed, raw $\Delta^{17}\text{O}$ values did not drift in any analyses of fine-grained phases and were not correlated with the drift of raw $\delta^{18}\text{O}$ values (see the Supporting Information section). Thus, we only report $\Delta^{17}\text{O}$ values for these eight fine-grained phase analyses (Fig. 4; Table 1).

The fine-grained domains in Z17 are free from epoxy (Fig. 2f), whereas in E36 and F39 analysis spots include epoxy resin that permeated porous fine-grained phases in the IDPs. Contamination by resins such as epoxy and acrylic is known to produce low $\delta^{18}\text{O}$ values along the terrestrial fractionation (TF) line (McKeegan et al. 2006; test analyses in this study; see the Supporting Information section), which is similar to the effects seen in the analyses of fine-grained phases. However, the secondary ion intensity of oxygen from epoxy resin must be more than an order of magnitude smaller than those of the IDP analyses, which were similar to or even greater than those of the olivine standard (see the Analytical Procedures section). Therefore, the low $\delta^{18}\text{O}$ values cannot be readily explained by epoxy alone. We speculate that ion bombardment of the silicate–epoxy mixture at the nanometer scale results in instrumental mass fractionation that is different from silicates.

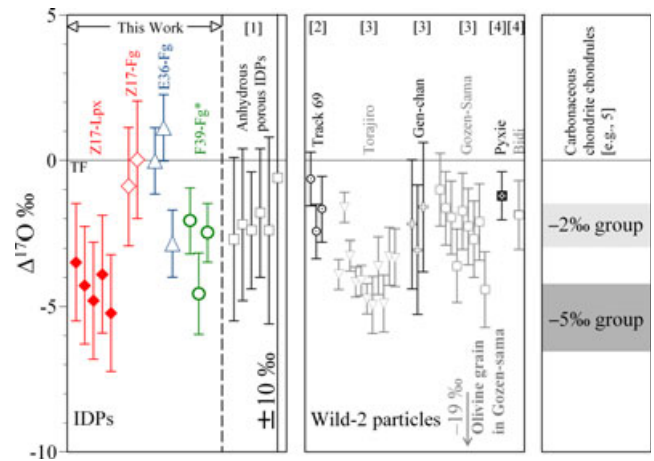


Fig. 4. Oxygen isotope ratios of the three IDPs (L2005 E36, F39, and Z17) are plotted as deviations from the terrestrial fractionation (TF) line ($\Delta^{17}\text{O} = \delta^{17}\text{O} - 0.52 \times \delta^{18}\text{O}$). The $\Delta^{17}\text{O}$ values of ferromagnesian silicate particles from comet Wild 2 and ferromagnesian silicates in anhydrous IDPs are shown for comparison: [1] Aléon et al. (2009), [2] McKeegan et al. (2006), and [3] Nakamura et al. (2008). Average $\Delta^{17}\text{O}$ values of two Wild 2 particles (Pyxie and Bidi) are also shown for comparison: [4] Nakashima et al. (2011a). Two chondrule groups having distinct $\Delta^{17}\text{O}$ values of -5‰ and -2‰ from Acfer 094 are shown for comparison: [5] Ushikubo et al. (2011). $\Delta^{17}\text{O}$ values of F39-Fg need to be treated with caution, because of large hydride corrections for the fine-grained phases (Table 1).

The $\Delta^{17}\text{O}$ values of two analyses in the fine-grained dense domain in Z17 are approximately 0‰ , which is different from those in the coarse low-Ca pyroxene grains in the same IDP. Therefore, Z17 must consist of grains with heterogeneous oxygen isotope ratios. The $\Delta^{17}\text{O}$ values of three analyses of E36 are slightly variable, showing one data at $-2.8 \pm 1.1\text{‰}$ and two others at 0‰ to $+1\text{‰}$. The $\Delta^{17}\text{O}$ values of three analyses of F39 show values approximately -3‰ , although one of them has larger analytical errors of 1.4‰ due to hydride corrections as high as 7‰ (Table 1). Possible explanations for the relatively high hydride contribution may be adsorbed water on the fine-grained phases that have large surface area and/or permeated epoxy. The magnitude of the $^{16}\text{O}^1\text{H}^-$ peak was recorded after each SIMS analysis for hydride correction (see Heck et al. 2010), so that we did not know the hydride contribution to $^{17}\text{O}^-$ during the SIMS analysis. The large hydride correction (7‰) might account for the low $\Delta^{17}\text{O}$ value of -4.6‰ in F39 (i.e., overcorrection), or the hydride contribution might have been higher than 7‰ during the analysis, which results in lower $\Delta^{17}\text{O}$ value than the current value (i.e., undercorrection). The same might be true for the spot with the $\Delta^{17}\text{O}$ value of -2.1‰ and 4‰ hydride correction in F39 (Table 1). These two data with 4‰ and 7‰ hydride corrections are needed to be treated

with caution. However, it should be noted that the $\Delta^{17}\text{O}$ values of the three IDPs are not correlated with the magnitude of the hydride correction (Table 1).

DISCUSSION

Similarity of $\Delta^{17}\text{O}$ Values Between Anhydrous IDPs and Wild 2 Particles

In Fig. 4, $\Delta^{17}\text{O}$ values of three IDPs obtained in this study are compared to those in anhydrous porous IDPs and ferromagnesian Wild 2 particles from previous studies. Aléon et al. (2009) reported oxygen three-isotope analyses of crystalline silicates in porous IDPs containing micrometer to submicrometer grains, which were pressed into gold foils and analyzed using approximately 10 μm spots. Their data mainly cluster at $\Delta^{17}\text{O} = -2\text{‰}$, although uncertainties of individual data ($\geq 2\text{‰}$) are somewhat larger than for the present study. Data from several ferromagnesian Wild 2 particles have been reported (McKeegan et al. 2006; Nakamura et al. 2008; Nakashima et al. 2011a) that show $\Delta^{17}\text{O}$ values ranging from -5‰ to -1‰ (Fig. 4), except for relict olivine in particle Gozen-sama (track 35) which has $\Delta^{17}\text{O}$ values as low as -19‰ . The $\Delta^{17}\text{O}$ values of the three anhydrous IDPs in the present study have a range from -5‰ to $+1\text{‰}$ (Fig. 4), which overlaps with ferromagnesian Wild 2 particles and crystalline silicates in anhydrous IDPs reported in the literature. By contrast, two GEMS-rich IDPs reported by Aléon et al. (2009) showed a wider spread in $\Delta^{17}\text{O}$ values of -9.3‰ and $+3.0\text{‰}$. GEMS were not identified from the fine-grained phases of the three IDPs in this work, which may explain the narrower range of $\Delta^{17}\text{O}$ values compared to those in Aléon et al. (2009). As mentioned by Nakamura et al. (2008), the oxygen three-isotope data from Wild 2 particles overlap with those of chondrules in primitive carbonaceous chondrites, which show a range of $\Delta^{17}\text{O}$ values mainly from approximately -6‰ to 0‰ (Krot et al. 2006a; Rudraswami et al. 2011; Tenner et al. 2011; Ushikubo et al. 2011). Nakamura et al. (2008) suggested that crystalline silicate particles in Wild 2 are chondrules that originally formed in the inner solar system and were transported to the outer solar nebula where comet Wild 2 formed.

Internal Isotope Heterogeneity Between Coarse- and Fine-Grained Domains of Z17

Data from coarser low-Ca pyroxene grains in Z17 have an average $\Delta^{17}\text{O}$ value of $-4.3 \pm 0.9\text{‰}$, which is close to the lower end of the $\Delta^{17}\text{O}$ variation for the Wild 2 particles in Fig. 4. This value is systematically lower than that of anhydrous porous IDP data reported by

Aléon et al. (2009). The coarse low-Ca pyroxene grains in Z17 are enclosed by a fine-grained domain with $\Delta^{17}\text{O}$ of approximately 0‰ (Fig. 4). Negative $\Delta^{17}\text{O}$ values are common for cometary dust particles (Fig. 4), whereas $\Delta^{17}\text{O}$ values close to 0‰ are rarely seen. If this IDP was pressed into gold foil for SIMS analyses, as in the case of previous IDP studies (McKeegan 1987; Aléon et al. 2009), coarse low-Ca pyroxene would have been crushed into submicrometer fragments and mixed with fine-grained domains. In this case, the two distinct $\Delta^{17}\text{O}$ values from coarse low-Ca pyroxene and the fine-grained dense domain would not have been identified by the SIMS analyses. The in-situ oxygen isotope analysis of IDP samples with polished flat surfaces was a key to success in detecting few-per mil isotope heterogeneity at the micrometer scale.

There are three possible explanations for isotope heterogeneity in the anhydrous IDP Z17: (1) dehydration of hydrous minerals, (2) oxygen isotope exchange with Earth's atmosphere during atmospheric entry, and (3) intrinsic oxygen isotope heterogeneity. Here, we discuss these three possible explanations.

Hydrous IDPs show $\Delta^{17}\text{O}$ values of approximately 0‰ with $\delta^{18}\text{O}$ of $\geq +4\text{‰}$ (Aléon et al. 2009), which spans the range of data from the fine-grained dense domains in Z17. However, Z17 is an anhydrous IDP (Zolensky and Barrett 1994). Dehydrated carbonaceous chondrites show high $\delta^{18}\text{O}$ values up to $+22\text{‰}$ along the TF line due to dehydration of hydrous minerals (Clayton and Mayeda 1999). Matrajt et al. (2006) reported oxygen three-isotope ratios of unmelted micrometeorites that are free from hydrous phases, having $\Delta^{17}\text{O}$ values of approximately 0‰ with high $\delta^{18}\text{O}$ from $+3\text{‰}$ to $+60\text{‰}$. Based on the high $\delta^{18}\text{O}$ values, which have never been observed in anhydrous silicates in meteorites, Matrajt et al. (2006) suggested that the unmelted micrometeorites might have derived from thermally metamorphosed carbonaceous chondritic asteroids that had not been collected as meteorites. It is possible that the fine-grained dense domain in Z17 with $\Delta^{17}\text{O} \sim 0\text{‰}$ is related to the source materials of the unmelted micrometeorites studied by Matrajt et al. (2006). However, the main problem with interpreting the fine-grained domain in Z17 to be a dehydrated carbonaceous chondrite is an absence of pores between submicrometer silicate and metallic phases (Fig. 2g). Carbonaceous chondrites that experienced dehydration show pores between silicate and metallic phase, which were produced by shrinkage of silicate during conversion from phyllosilicate to anhydrous silicates (olivine and pyroxene) and/or shrinkage of metallic phases (Nakamura 2005, 2006). Z17 shows no pore space between submicrometer silicate and FeNi metal, and thus, oxygen isotope ratios of fine-grained dense domains in Z17 may not be explained by

dehydration after aqueous alteration of a chondritic parent body.

High $\delta^{18}\text{O}$ values on the TF line have also been reported from melted micrometeorites (Yada et al. 2005), where they result from oxygen isotope exchange with Earth's atmosphere during the atmospheric entry. The maximum heating temperature of IDPs during atmospheric entry is estimated to be 1600 °C (Flynn 1989). The grain size in the fine-grained domain in Z17 is assumed to be 100 nm (see the Results section). The diffusion coefficient of oxygen isotope in olivine at 1600 °C is approximately $10^{-17} \text{ m}^2 \text{ s}^{-1}$ (Gerard and Jaoul 1989), whereas that in pyroxene is approximately $10^{-16} \text{ m}^2 \text{ s}^{-1}$ at 1600 °C (Ryerson and McKeegan 1994). The heating durations for oxygen isotope exchange in olivine and pyroxene at 1600 °C are required to be approximately 300 and 30 s, respectively. Modeling by Love and Brownlee (1991, 1994) shows that IDPs spend 1–2 s at around their peak temperatures, and therefore a heating duration of approximately 300 and 30 s during atmospheric entry is unlikely. Thus, distinct $\Delta^{17}\text{O}$ values between fine-grained domains and coarse low-Ca pyroxene in Z17 cannot be explained by oxygen isotope exchange between the fine-grained domains and Earth's atmosphere.

Another possibility is the presence of small quantity of materials with high $\Delta^{17}\text{O}$ values, such as COS-like dust or presolar grains (Messenger et al. 2003; Sakamoto et al. 2007; Keller and Messenger 2011), in the fine-grained domains. For example, addition of approximately 5% of COS with $\Delta^{17}\text{O} \sim +80\text{‰}$ (Sakamoto et al. 2007) in the fine-grained dense domains would be enough to explain the difference between $\Delta^{17}\text{O}$ values of coarse pyroxene and fine-grains phase in Z17. However, the indistinguishable $\Delta^{17}\text{O}$ values from two analyses in the fine-grained dense domains are difficult to explain unless these materials with distinct oxygen isotope ratios distributed homogeneously. As mentioned earlier, electron microprobe analyses of Z17 indicate that grains in the IDP are not equilibrated (Zolensky and Barrett 1994); thus, distinct oxygen isotope ratios would not be homogenized in the fine-grained dense domains. We conclude that anhydrous IDP Z17 preserves intrinsic oxygen isotope heterogeneity, but the source of this heterogeneity remains unknown. Further study on anhydrous IDPs might provide some clues.

Anhydrous Porous IDPs

We selected two of the anhydrous porous IDPs E36 and F39 because they contain relatively large grains (up to 3 μm) that could be analyzed using 1–2 μm SIMS spots. Unfortunately, due to difficulty in sample preparation and accuracy of aiming the SIMS spots, we were not able to analyze clean single mineral grains in

these IDPs. This resulted in analyses of multiple minerals, and derived values are the averaged isotope ratios of the minerals. Even if the minerals had heterogeneous oxygen isotope ratios, the heterogeneity would become less recognizable. However, three analyses in E36 display a hint of internal heterogeneity, with $\Delta^{17}\text{O}$ values of -3‰ and $+1\text{‰}$. Such internal per mil-level heterogeneity has not been previously identified in studies, in which IDPs were pressed into gold foil and analyzed as bulk grains. Since submicrometer grains could be lost after the in situ oxygen isotope analysis by SIMS, careful petrologic observation is needed to understand oxygen isotope systematics in anhydrous IDPs.

As mentioned earlier, anhydrous porous IDPs are generally considered to be of cometary origin (Bradley 2003; see the Introduction). Although anhydrous porous IDPs and Wild 2 crystalline silicate particles show similar chemical and isotopic signatures (McKeegan et al. 2006; Zolensky et al. 2006; Nakamura et al. 2008; Aléon et al. 2009), oxygen isotope ratios of Wild 2 particles reported so far were from particles with coarse-grained (\geq few μm) igneous textures, but not submicrometer crystalline silicates. This is possibly due to the loss of fine-grained particles by impact-generated melting with the silica aerogel capture media. Thus, anhydrous porous IDPs provide critical information on the fine-grained crystalline silicate particles that are missing from the Wild 2 samples. The range of $\Delta^{17}\text{O}$ values from E36 and F39 is generally consistent with that of Wild 2 terminal particles (McKeegan et al. 2006; Nakamura et al. 2008; Nakashima et al. 2011a). Based on these data, we further speculate that crystalline silicates in comets may have oxygen isotope ratios falling inside the range from -5‰ to $+1\text{‰}$ in $\Delta^{17}\text{O}$, independent of crystal sizes (nanometer scale vs. micrometer scale) and textures (loose aggregates vs. coarse-grained particles).

Oxygen Isotope Reservoirs in Outer Asteroid Belt and Beyond

The range of $\Delta^{17}\text{O}$ values observed from Wild 2 particles and anhydrous IDPs is similar to that observed in chondrules in carbonaceous chondrites. Recently, several studies indicate that each chondrite group shows specific distribution patterns of $\Delta^{17}\text{O}$ values among chondrules (e.g., Libourel and Chaussidon 2011; Ushikubo et al. 2011). For Acfer 094 (ungrouped), Yamato-81020 (CO3.0), and Allende (CV3), the $\Delta^{17}\text{O}$ values show a bimodal distribution at approximately -5‰ and -2‰ , with the majority at -5‰ (Fig. 4) (Rudraswami et al. 2011; Tenner et al. 2011; Ushikubo et al. 2011). In metal-rich carbonaceous chondrites, such as CR, CH, and CB, the majority of chondrules show $\Delta^{17}\text{O}$ values at -2‰ (Krot et al. 2006b, 2010;

Nakashima et al. 2010). Furthermore, small fractions of chondrules in carbonaceous chondrites show positive $\Delta^{17}\text{O}$ values as high as $+5\text{‰}$ (Krot et al. 2010; Nakashima et al. 2010). According to Fig. 4, both Wild 2 particles and anhydrous IDPs seem to show peaks at $\Delta^{17}\text{O}$ values of -2‰ . Based on this, Ushikubo et al. (2011) suggested that oxygen isotopes in the outer solar system might be dominated by $\Delta^{17}\text{O}$ values of -2‰ , including outer asteroid belt and comets. Our new data from anhydrous IDPs seem to show micrometer-scale internal heterogeneity similar to the range observed from major chondrules in various types of carbonaceous chondrites, although their bulk average value would be close to -2‰ (Table 1). Similar $\Delta^{17}\text{O}$ values of -2‰ are frequently observed in Wild 2 terminal particles, probably because melting of heterogeneous precursor materials would average out the oxygen isotope heterogeneity with peak $\Delta^{17}\text{O}$ values at -2‰ . More data with high precision and high spatial resolution will reveal oxygen isotope heterogeneity at the few-per mil level in tiny particles such as Wild 2 particles and IDPs, which is necessary for a complete understanding of oxygen isotope reservoirs in the outer solar system objects.

Anhydrous IDPs cannot readily be explained as deriving from chondrule fragments, given the frequent presence of GEMS grains, which may be nonequilibrium condensates in the solar nebula based on oxygen isotope and chemical analyses (Keller and Messenger 2011). Crystalline silicates in comets have been suggested to have formed by annealing of amorphous silicate grains in the hot inner solar nebula followed by transportation outward toward the outer solar nebula (Hallenbeck et al. 2000; Nuth et al. 2000). Rather than crystallization from amorphous solids, another possible origin of crystalline cometary silicates is direct condensation from high temperature gas, as suggested by the presence in anhydrous IDPs of enstatite whiskers (and platelets) and low-iron, manganese-rich forsterite (Bradley et al. 1983; Klöck et al. 1989). We infer from our new oxygen isotope data of anhydrous IDPs as well as the data of Aléon et al. (2009) that the isotope reservoirs from which both cometary crystalline silicates and carbonaceous chondrite chondrules formed had similar oxygen isotope ratios, although these reservoirs could have been separated in time and space during the early evolution of the solar system.

Among meteoritic components, unaltered matrix in chondrites, which consists mainly of amorphous and submicrometer crystalline silicates (plus Fe-sulfides), is most similar to anhydrous IDPs (Greshake 1997; Bradley 2003; Abreu and Brearley 2010). Fine-grained matrix in carbonaceous chondrites shows negative $\Delta^{17}\text{O}$ values, similar to that in the anhydrous IDPs, although their $\delta^{18}\text{O}$ and $\delta^{17}\text{O}$ are often mass fractionated to higher

values due to low-temperature rock–fluid interaction (Clayton and Mayeda 1999). Unfortunately, there is no oxygen isotope data at a few-per mil level precision from unaltered matrix of carbonaceous chondrites, which will be needed in the future to further elucidate whether there is a genetic link between anhydrous IDPs and chondritic matrix.

CONCLUSIONS

Oxygen isotope analyses of three anhydrous IDPs (E36, F39, and Z17) show $\Delta^{17}\text{O}$ values that range from -5‰ to $+1\text{‰}$. Two of the IDPs (E36 and Z17) show internal heterogeneity of oxygen isotope ratios at the micrometer-scale (Fig. 4), which was enabled by high-precision oxygen isotope analysis using an approximately $2\ \mu\text{m}$ primary beam on polished flat surfaces. The $\Delta^{17}\text{O}$ values of the IDPs overlap with those of ferromagnesian silicate particles from comet Wild 2 and anhydrous porous IDPs (McKeegan et al. 2006; Nakamura et al. 2008; Aléon et al. 2009; Nakashima et al. 2011a). If anhydrous IDPs represent fine-grained particles from comets that are missing from Wild 2 particles due to collection bias, it is implied that ferromagnesian crystalline silicates in comets have similar oxygen isotope ratios independent of crystal sizes (nanometer scale vs. micrometer scale) and textures (loose aggregates vs. coarse-grained particles). The range of $\Delta^{17}\text{O}$ values of the three anhydrous IDPs also overlaps with that of chondrules in carbonaceous chondrites (Krot et al. 2006a), suggesting a genetic link between cometary dust particles (Wild 2 particles and most anhydrous IDPs) and carbonaceous chondrite chondrules (see also Ushikubo et al. 2011).

Acknowledgments—Thoughtful comments from T. Stephan, J. Aléon, S. Messenger, and C. Floss improved the quality of this manuscript significantly. The authors thank R. K. Noll for help with FE-SEM observation, P. E. Brown for lending a high magnification objective lens for optical microscope, H. Xu for allowing using a polarizing microscope, and J. Kern for SIMS support. This work is supported by the NASA LARS program (NK, NNX09AC30G). WiscSIMS is partly supported by NSF-EAR (0319230, 0744079). M. Z. was supported by NASA's Cosmochemistry and Laboratory Analysis of Returned Samples Programs.

Editorial Handling—Dr. Christine Floss

REFERENCES

- Abreu N. M. and Brearley A. J. 2010. Early solar system processes recorded in the matrices of two highly pristine

- CR3 carbonaceous chondrites, MET 00426 and QUE 99177. *Geochimica et Cosmochimica Acta* 74:1146–1171.
- Aléon J., Engrand C., Leshin L. A., and McKeegan K. D. 2009. Oxygen isotopic composition of chondritic interplanetary dust particles: A genetic link between carbonaceous chondrites and comets. *Geochimica et Cosmochimica Acta* 73:4558–4575.
- Bradley J. P. 1994. Chemically anomalous, preaccretionally irradiated grains in interplanetary dust from comets. *Nature* 265:925–929.
- Bradley J. P. 1995. GEMS and interstellar silicate grains (abstract). 26th Lunar and Planetary Science Conference. pp. 159–160.
- Bradley J. P. 2003. Interplanetary dust particles. In *Meteorites, comets, and planets*, edited by Holland H. D. and Turekian K. K. Treatise on Geochemistry, vol. 1. Amsterdam: Elsevier B.V. pp. 689–711.
- Bradley J. P., Brownlee D. E., and Veblen D. R. 1983. Pyroxene whiskers and platelets in interplanetary dust: Evidence of vapour phase growth. *Nature* 301:473–477.
- Bradley J. P., Wozniakiewicz P., and Ishii H. A. 2011. Constraints on the cosmochemical significance of element/Si ratios and oxygen isotopic compositions of GEMS from IDPs collected in silicone oil (abstract #1320). 42nd Lunar and Planetary Science Conference. CD-ROM.
- Brownlee D. E., Joswiak D. J., Schlutter D. J., Pepin R. O., Bradley J. P., and Love S. G. 1995. Identification of individual cometary IDP's by thermally stepped He release (abstract). 26th Lunar and Planetary Science Conference. pp. 183–184.
- Brownlee D., Tsou P., Aléon J., Alexander C. M. O' D., Araki T., Bajt S., Baratta G. A., Bastien R., Bland P., Bleuët P., Borg J., Bradley J. P., Brearley A., Brenker F., Brennan S., Bridges J. C., Browning N. D., Brucato J. R., Bullock E., Burchell M. J., Busemann H., Butterworth A., Chaussidon M., Chevront A., Chi M., Cintala M. J., Clark B. C., Clemett S. J., Cody G., Colangeli L., Cooper G., Cordier P., Daghlian C., Dai Z., D'Hendecourt L., Djouadi Z., Dominguez G., Duxbury T., Dworkin J. P., Ebel D. S., Economou T. E., Fakra S., Fairey S. A. J., Fallon S., Ferrini G., Ferroir T., Fleckenstein H., Floss C., Flynn G., Franchi I. A., Fries M., Gainsforth Z., Gallien J.-P., Genge M., Gilles M. K., Gillet Ph., Gilmour J., Glavin D. P., Gounelle M., Grady M. M., Graham G. A., Grant P. G., Green S. F., Grossemy F., Grossman L., Grossman J. N., Guan Y., Hagiya K., Harvey R., Heck P., Herzog G. F., Hoppe P., Hörz F., Huth J., Hutcheon I. D., Ignatyev K., Ishii H., Ito M., Jacob D., Jacobsen C., Jacobsen S., Jones S., Joswiak D., Jurewicz A., Kearsley A. T., Keller L. P., Khodja H., Kilcoyne A. L. D., Kissel J., Krot A., Langenhorst F., Lanzirotti A., Le L., Leshin L. A., Leitner J., Lemelle L., Leroux H., Liu M.-C., Luening K., Lyon I., MacPherson G., Marcus M. A., Marhas K., Marty B., Matrajt G., McKeegan K., Meibom A., Mennella V., Messenger K., Messenger S., Mikouchi T., Mostefaoui S., Nakamura T., Nakano T., Newville M., Nittler L. R., Ohnishi I., Ohsumi K., Okudaira K., Papanastassiou D. A., Palma R., Palumbo M. E., Pepin R. O., Perkins D., Perronnet M., Pianetta P., Rao W., Rietmeijer F. J. M., Robert F., Rost D., Rotundi A., Ryan R., Sandford S. A., Schwandt C. S., See T. H., Schlutter D., Sheffield-Parker J., Simionovici A., Simon S., Sittinsky I., Snead C. J., Spencer M. K., Stadermann F. J., Steele A., Stephan T., Stroud R., Susini J., Sutton S. R., Suzuki Y., Taheri M., Taylor S., Teslich N., Tomeoka K., Tomioka N., Toppani A., Trigo-Rodríguez J. M., Troadec D., Tsuchiyama A., Tuzzolino A. J., Tyliczszak T., Uesugi K., Velbel M., Vellenga J., Vicenzi E., Vincze L., Warren J., Weber I., Weisberg M., Westphal A. J., Wirick S., Wooden D., Wopenka B., Wozniakiewicz P., Wright I., Yabuta H., Yano H., Young E. D., Zare R. N., Zega T., Ziegler K., Zimmermann L., Zinner E., and Zolensky M. 2006. Comet 81P/Wild 2 under a microscope. *Science* 314:1711–1716.
- Ciesla F. J. 2007. Outward transport of high-temperature materials around the midplane of the solar nebula. *Science* 318:613–615.
- Clayton R. N. 1993. Oxygen isotopes in meteorites. *Annual Review of Earth and Planetary Sciences* 21:115–149.
- Clayton R. N. and Mayeda T. K. 1999. Oxygen isotope studies of carbonaceous chondrites. *Geochimica et Cosmochimica Acta* 63:2089–2104.
- Clayton R. N., Onuma N., Grossman L., and Mayeda T. K. 1977. Distribution of the pre-solar component in Allende and other carbonaceous chondrites. *Earth and Planetary Science Letters* 34:209–224.
- Flynn G. J. 1989. Atmospheric entry heating: A criterion to distinguish between asteroidal and cometary sources of interplanetary dust. *Icarus* 77:287–310.
- Gerard O. and Jaoul O. 1989. Oxygen diffusion in San Carlos olivine. *Journal of Geophysical Research* 94:4119–4128.
- Greshake A. 1997. The primitive matrix components of the unique carbonaceous chondrite Acfer 094: A TEM study. *Geochimica et Cosmochimica Acta* 61:437–452.
- Hallenbeck S. L., Nuth J. A., and Nelson R. N. 2000. Evolving optical properties of annealing silicate grains: From amorphous condensate to crystalline mineral. *The Astrophysical Journal* 535:247–255.
- Heck P. R., Ushikubo T., Schmitz B., Kita N. T., Spicuzza M. J., and Valley J. W. 2010. A single asteroidal source for extraterrestrial Ordovician chromite grains from Sweden and China: High-precision oxygen three-isotope SIMS analysis. *Geochimica et Cosmochimica Acta* 74:497–509.
- Jackson A. A. and Zook H. A. 1992. Orbital evolution of dust particles from comets and asteroids. *Icarus* 97:70–84.
- Joswiak D. J., Brownlee D. E., Pepin R. O., and Schlutter D. J. 2000. Characteristics of asteroidal and cometary IDPs obtained from stratospheric collectors: Summary of measured He release temperatures, velocities and descriptive mineralogy (abstract #1500). 31st Lunar and Planetary Science Conference. CD-ROM.
- Keller L. P. and Messenger S. 2011. On the origins of GEMS grains. *Geochimica et Cosmochimica Acta* 75:5336–5365.
- Kita N. T., Ushikubo T., Fu B., and Valley J. W. 2009. High precision SIMS oxygen isotope analysis and the effect of sample topography. *Chemical Geology* 264:43–57.
- Kita N. T., Nagahara H., Tachibana S., Tomomura S., Spicuzza M. J., Fournelle J. H., and Valley J. W. 2010. High precision SIMS oxygen three isotope study of chondrules in LL3 chondrites: Role of ambient gas during chondrule formation. *Geochimica et Cosmochimica Acta* 74:6610–6635.
- Klöck W., Thomas K. L., McKay D. S., and Palme H. 1989. Unusual olivine and pyroxene composition in interplanetary dust and unequilibrated ordinary chondrites. *Nature* 339:126–128.
- Kobayashi S., Imai H., and Yurimoto H. 2003. New extreme ¹⁶O-rich reservoir in the early solar system. *Geochemical Journal* 37:663–669.

- Krot A. N., Yurimoto H., McKeegan K. D., Leshin L., Chaussidon M., Libourel G., Yoshitake M., Huss G. R., Guan Y., and Zanda B. 2006a. Oxygen isotopic compositions of chondrules: Implications for evolution of oxygen isotopic reservoirs in the inner solar nebula. *Chemie der Erde* 66:249–276.
- Krot A. N., Libourel G., and Chaussidon M. 2006b. Oxygen isotope compositions of chondrules in CR chondrites. *Geochimica et Cosmochimica Acta* 70:767–779.
- Krot A. N., Nagashima K., Yoshitake M., and Yurimoto H. 2010. Oxygen isotopic compositions of chondrules from the metal-rich chondrites Isheyevo (CH/CB_b), MAC 02675 (CB_b) and QUE 94627 (CB_b). *Geochimica et Cosmochimica Acta* 74:2190–2211.
- Libourel G. and Chaussidon M. 2011. Oxygen isotopic constraints on the origin of Mg-rich olivines from chondritic meteorites. *Earth and Planetary Science Letters* 301:9–21.
- Love S. G. and Brownlee D. E. 1991. Heating and thermal transformation of micrometeorites entering the Earth's atmosphere. *Icarus* 89:26–43.
- Love S. G. and Brownlee D. E. 1993. A direct measurement of the terrestrial mass accretion rate of cosmic dust. *Science* 262:550–553.
- Love S. G. and Brownlee D. E. 1994. Peak atmospheric entry temperatures of micrometeorites. *Meteoritics* 29:69–70.
- Lyons J. R. and Young E. D. 2005. CO self-shielding as the origin of oxygen isotope anomalies in the early solar nebula. *Nature* 435:317–320.
- Matrajt G., Guan Y., Leshin L., Taylor S., Genge M., Joswiak D., and Brownlee D. 2006. Oxygen isotope measurements of individual unmelted Antarctic micrometeorites. *Geochimica et Cosmochimica Acta* 70:4007–4018.
- McKeegan K. D. 1987. Oxygen isotopes in refractory stratospheric dust particles: Proof of extraterrestrial origin. *Science* 237:1468–1471.
- McKeegan K. D., Aléon J., Bradley J., Brownlee D., Busemann H., Butterworth A., Chaussidon M., Fallon S., Floss C., Gilmour J., Gounelle M., Graham G., Guan Y., Heck P. R., Hoppe P., Hutcheon I. D., Huth J., Ishii H., Ito M., Jacobsen S. B., Kearsley A., Leshin L. A., Liu M.-C., Lyon I., Marhas K., Marty B., Matrajt G., Meibom A., Messenger S., Mostefaoui S., Mukhopadhyay S., Nakamura-Messenger K., Nittler L., Palma R., Pepin R. O., Papanastassiou D. A., Robert F., Schlutter D., Snead C. J., Stadermann F. J., Stroud R., Tsou P., Westphal A., Young E. D., Ziegler K., Zimmermann L., and Zinner E. 2006. Isotopic compositions of cometary matter returned by Stardust. *Science* 314:1724–1728.
- McKeegan K. D., Kallio A. P., Heber V. S., Jarzebinski G., Mao P. H., Coath C. D., Kunihiro T., Wiens R. C., Nordholt J. E., Moses R. W. Jr., Reisenfeld D. B., Jurewicz A. J. G., and Burnett D. S. 2011. The oxygen isotopic composition of the Sun inferred from captured solar wind. *Science* 332:528–532.
- Messenger S. 2000. Identification of molecular-cloud material in interplanetary dust particles. *Nature* 404: 968–971.
- Messenger S. 2002. Opportunities for the stratospheric collection of dust from short-period comets. *Meteoritics & Planetary Science* 37:1491–1505.
- Messenger S. 2011. Stratospheric collection of dust from comet 73P/Schwassmann-Wachmann 3 (abstract #2158). 42nd Lunar and Planetary Science Conference. CD-ROM.
- Messenger S., Keller L. P., Stadermann F. J., Walker R. M., and Zinner E. 2003. Samples of stars beyond the solar system: Silicate grains in interplanetary dust. *Science* 300:105–108.
- Nakamura T. 2005. Post-hydration thermal metamorphism of carbonaceous chondrites. *Journal of Mineralogical and Petrological Sciences* 100:260–272.
- Nakamura T. 2006. Yamato 793321 CM chondrite: Dehydrated regolith material of a hydrous asteroid. *Earth and Planetary Science Letters* 242:26–38.
- Nakamura T., Noguchi T., Tsuchiyama A., Ushikubo T., Kita N. T., Valley J. W., Zolensky M. E., Kakazu Y., Sakamoto K., Mashio E., Uesugi K., and Nakano T. 2008. Chondrule-like objects in short-period comet 81P/Wild 2. *Science* 321:1664–1667.
- Nakamura T., Noguchi T., Tsuchiyama A., Ushikubo T., Kita N. T., Valley J. W., Takahata N., Sano Y., Zolensky M. E., Kakazu Y., Uesugi K., and Nakano T. 2009. Additional evidence for the presence of chondrules in comet 81P/Wild 2 (abstract). *Meteoritics & Planetary Science* 44:A153.
- Nakashima D., Kimura M., Yamada K., Noguchi T., Ushikubo T., and Kita N. T. 2010. Study of chondrules in CH chondrites—I: Oxygen isotope ratios of chondrules (abstract). *Meteoritics & Planetary Science* 45:A148.
- Nakashima D., Ushikubo T., Zolensky M. E., Weisberg M. K., Joswiak D. J., Brownlee D. E., Matrajt G., and Kita N. T. 2011a. High precision oxygen three isotope analysis of Wild 2 particles and anhydrous chondritic interplanetary dust particles (abstract #1240). 42nd Lunar and Planetary Science Conference. CD-ROM.
- Nakashima D., Ushikubo T., Rudraswami N. G., Kita N. T., Valley J. W., and Nagao K. 2011b. Ion microprobe analyses of oxygen three-isotope ratios of chondrules from the Sayh al Uhaymir 290 chondrite using a multiple-hole disk. *Meteoritics & Planetary Science* 46:857–874.
- Nuth J. A., Hill H. G. M., and Kletetschka G. 2000. Determining the ages of comets from the fraction of crystalline dust. *Nature* 406:275–276.
- Rudraswami N. G., Ushikubo T., Nakashima D., and Kita N. T. 2011. Oxygen isotope systematics of chondrules in Allende CV3 chondrite: High precision ion microprobe studies. *Geochimica et Cosmochimica Acta*. 75:7596–7611.
- Ryerson F. J. and McKeegan K. D. 1994. Determination of oxygen self-diffusion in åkermanite, anorthite, diopside, and spinel: Implications for oxygen isotopic anomalies and the thermal histories of Ca-Al-rich inclusions. *Geochimica et Cosmochimica Acta* 58:3713–3734.
- Sakamoto N., Seto Y., Itoh S., Kuramoto K., Fujino K., Nagashima K., Krot A. N., and Yurimoto H. 2007. Remnants of the early solar system water enriched in heavy oxygen isotopes. *Science* 317:231–233.
- Tenner T. J., Ushikubo T., Kurahashi E., Kita N. T., and Nagahara H. 2011. Oxygen isotopic measurements of phenocrysts in chondrules from the primitive carbonaceous chondrite Yamato 81020: Evidence for two distinct oxygen isotope reservoirs (abstract #1426). 42nd Lunar and Planetary Science Conference. CD-ROM.
- Ushikubo T., Kimura M., Kita N. T., and Valley J. W. 2011. Primordial oxygen isotope reservoirs of the solar nebula recorded in chondrules in Acfer 094 carbonaceous chondrite (abstract #1183). 42nd Lunar and Planetary Science Conference. CD-ROM.

- Yada T., Nakamura T., Noguchi T., Matsumoto N., Kusakabe M., Hiyagon H., Ushikubo T., Sugiura N., Kojima H., and Takaoka N. 2005. Oxygen isotopic and chemical compositions of cosmic spherules collected from the Antarctic ice sheet: Implications for their precursor materials. *Geochimica et Cosmochimica Acta* 69:5789–5804.
- Young E. D. and Russell S. S. 1998. Oxygen reservoirs in the early solar nebula inferred from an Allende CAI. *Science* 282:452–455.
- Yurimoto H. and Kuramoto K. 2004. Molecular cloud origin for the oxygen isotope heterogeneity in the solar system. *Science* 305:1763–1766.
- Zolensky M. E. and Barrett R. A. 1994. Compositional variations of olivines and pyroxenes in chondritic interplanetary dust particles. *Meteoritics* 29:616–620.
- Zolensky M. E., Zega T. J., Yano H., Wirick S., Westphal A. J., Weisberg M. K., Weber I., Warren J. L., Velbel M. A., Tsuchiyama A., Tsou P., Toppani A., Tomioka N., Tomeoka K., Teslich N., Taheri M., Susini J., Stroud R., Stephan T., Stadermann F. J., Snead C. J., Simon S. B., Simionovici A., See T. H., Robert F., Rietmeijer F. J. M., Rao W., Perronnet M. C., Papanastassiou D. A., Okudaira K., Ohsumi K., Ohnishi I., Nakamura-Messenger K., Nakamura T., Mostefaoui S., Mikouchi T., Meibom A., Matrajt G., Marcus M. A., Leroux H., Lemelle L., Le L., Lanzirotti A., Langenhorst F., Krot A. N., Keller L. P., Kearsley A. T., Joswiak D., Jacob D., Ishii H., Harvey R., Hagiya K., Grossman L., Grossman J. N., Graham G. A., Gounelle M., Gillet P., Genge M. J., Flynn G., Ferroir T., Fallon S., Ebel D. S., Dai Z. R., Cordier P., Clark B., Chi M., Butterworth A. L., Brownlee D. E., Bridges J. C., Brennan S., Brearley A., Bradley J. P., Bleuet P., Bland P. A., and Bastien R. 2006. Mineralogy and petrology of comet 81P/Wild 2 nucleus samples. *Science* 314:1735–1739.

SUPPORTING INFORMATION

Additional supporting information may be found in the online version of this article:

Table S1: $\delta^{18}\text{O}$ values of mixed spots between San Carlos olivine and epoxy in various fractions measured with 10 μm spots (~ 2 nA).

Table S2: Raw SIMS measured oxygen isotope data of three anhydrous IDPs.

Please note: Wiley-Blackwell is not responsible for the content or functionality of any supporting materials supplied by the authors. Any queries (other than missing material) should be directed to the corresponding author for the article.
